Electronic Supplementary Material (ESI) for Journal of Materials Chemistry

Supporting Information

Giant dielectric permittivity of detonation-produced nanodiamond is caused by water

Stepan S. Batsanov, Sergei M. Gavrilkin, Andrei S. Batsanov, Konstantin B. Poyarkov, Inna I. Kulakova, David W. Johnson, Budhika G. Mendis

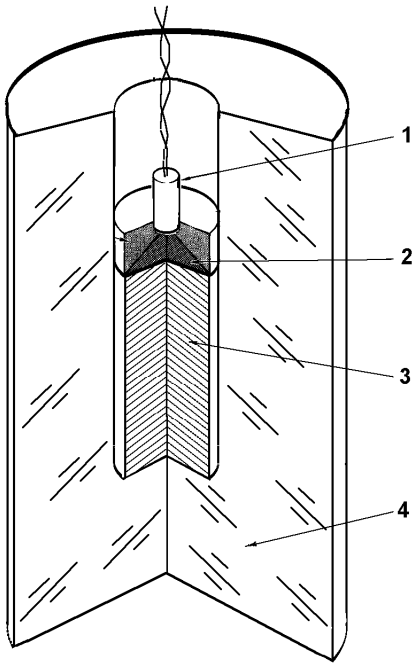

Figure S1. Explosive experiment setting for DND synthesis: (*1*) detonator, (*2*) generator of plane shock-wave, (*3*) TNT-RDX alloy, (*4*) ice shell. Reproduced with permission from: S. M. Gavrilkin, S. S. Batsanov, Yu. A. Gordopolov and A. S. Smirnov, *Propellants, Explosives, Pyrotechnics*, 2009, **34**, 469. Copyright 2009 John Wiley and Sons

Table S1. Langmuir and BET results

Experiment	sample mass (g)	BET model		*C*	Langmuir model	
		surface area *S* (m^2/g)	correlation coefficient[a]		surface area *S* (m^2/g)	correlation coefficient[a]
1	0.2238	180.89	0.9999832	113.04	288.70	0.993037
2	0.2238	180.58	0.9999695	115.50	246.87	0.997778
3	0.2238	180.56	0.9998793	134.68	267.69	0.999050
Low pressure	0.2144	168.96	0.9997691	279.11	190.88	0.998689

[a]Correlation coefficients of >0.999 are necessary for a good fit.

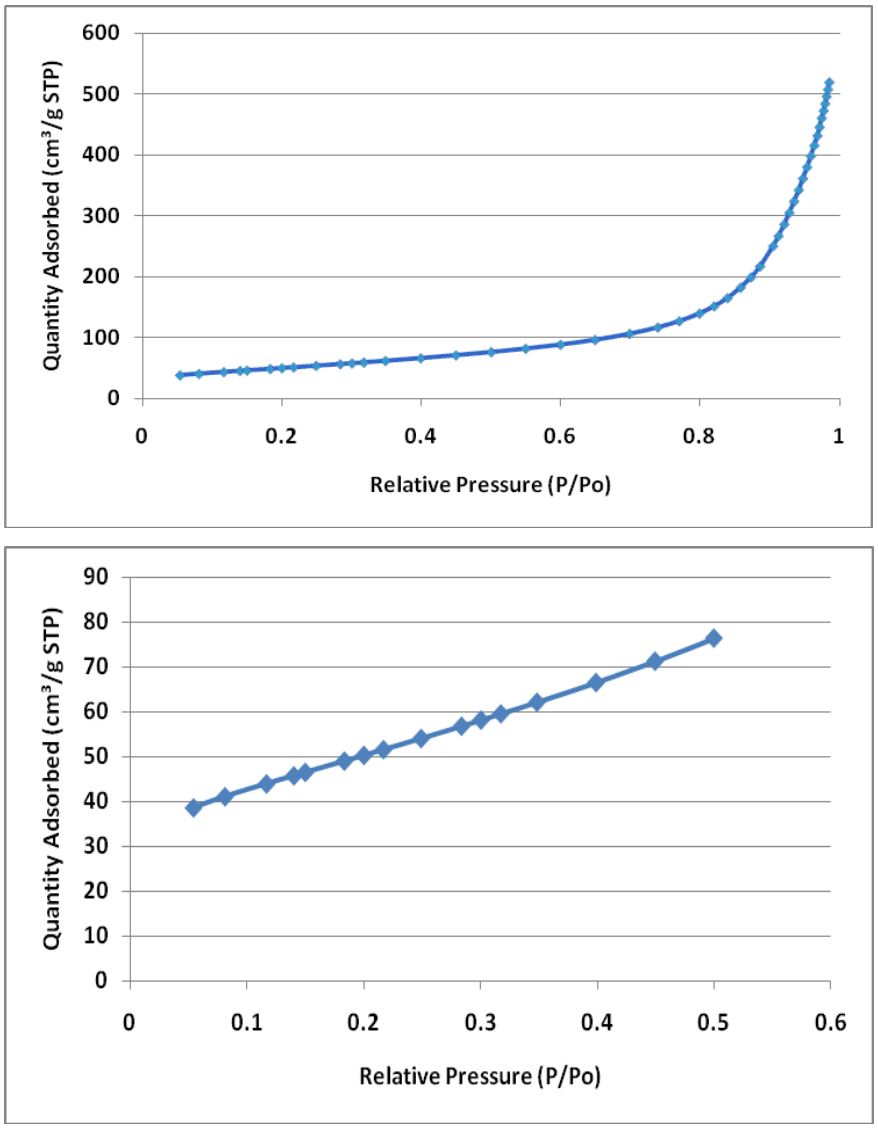

Figure S2. Absorption isotherm of DND **1** (top) and its low–medium relative pressure range

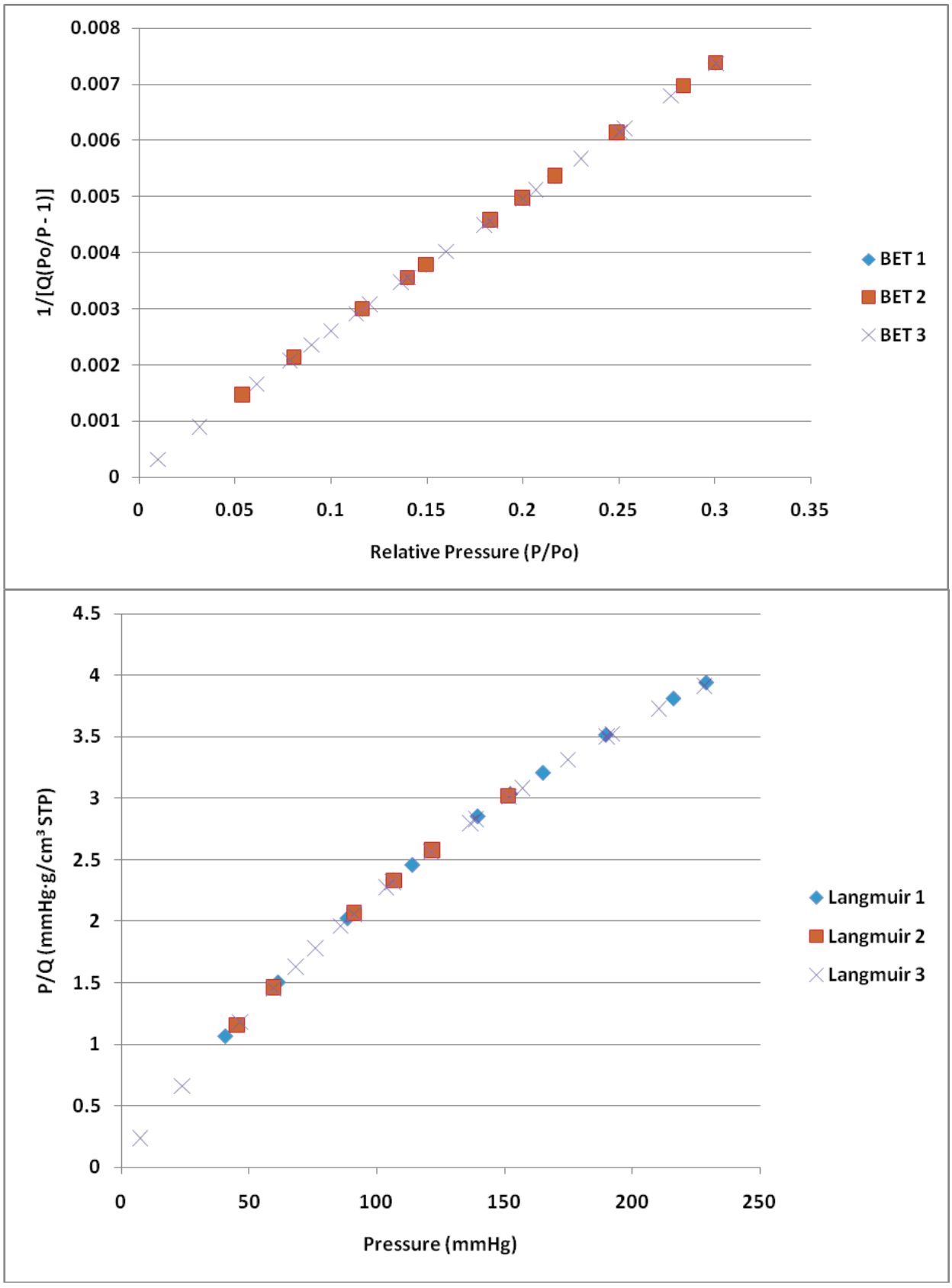

Figure S3. Surface area plots for BET (top) and Langmuir (bottom) models from 3 experiments

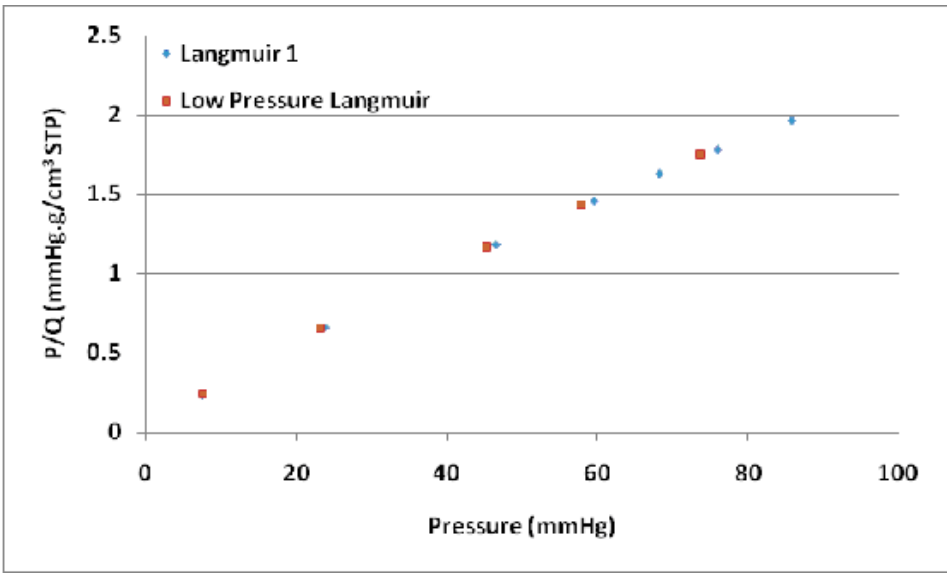

Figure S4. Langmuir surface area plots in experiment 1 and the low pressure experiment

Gas pycnometry protocol. The sample was weighed out into the sample cup, inserted into the pycnometer 10 cm^3 sample chamber, allowed to reach thermal equilibrium within the instrument (10 min) and then subjected to 50 purge cycles (He, 19.500 psig to 0 psig) to remove air and moisture from the chamber. The sample chamber pressure was increased to 19.500 psig, the chamber was then opened to a calibrated expansion volume. The pressure reading was then taken once the value was stable to≤0.005 psig/min and was used to calculate the sample volume.

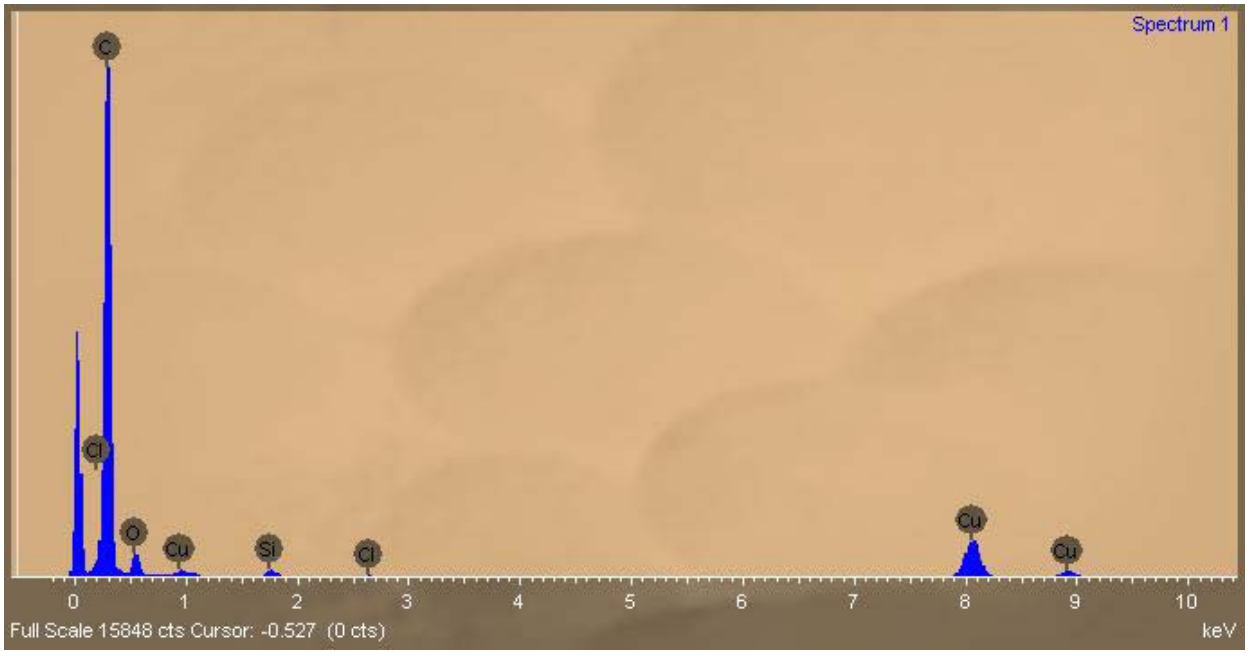

Figure S5. Energy-dispersive X-ray (EDX) spectrum of DND (**1**). Peaks other than carbon and oxygen originate from the sample holder.

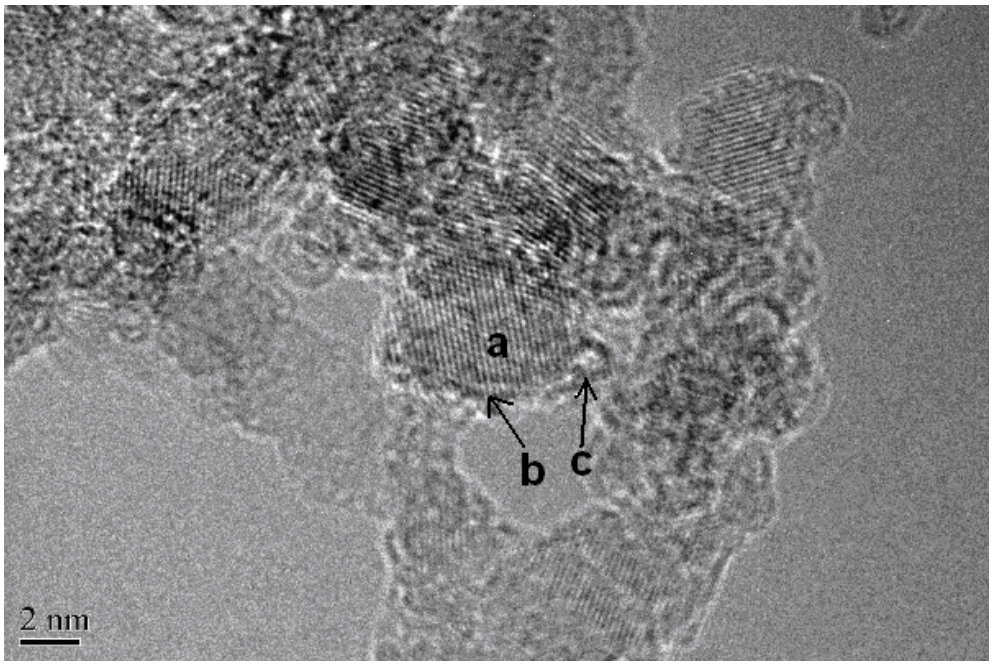

Figure S6. High-resolution TEM image of a freshly-prepared DND particle suspended over vacuum: (a) diamond core, (b) non-diamond shell, (c) spherical features of ca. 1 nm diameter may be interpreted as a fullerene cage.

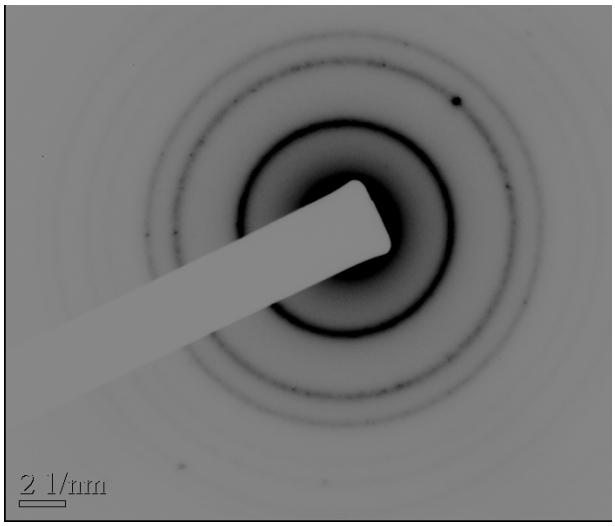

Figure S7. Electron diffraction pattern of freshly-prepared DND. Spots originate from a single 20 nm particle, rings from the predominant 4 – 5 nm particles.

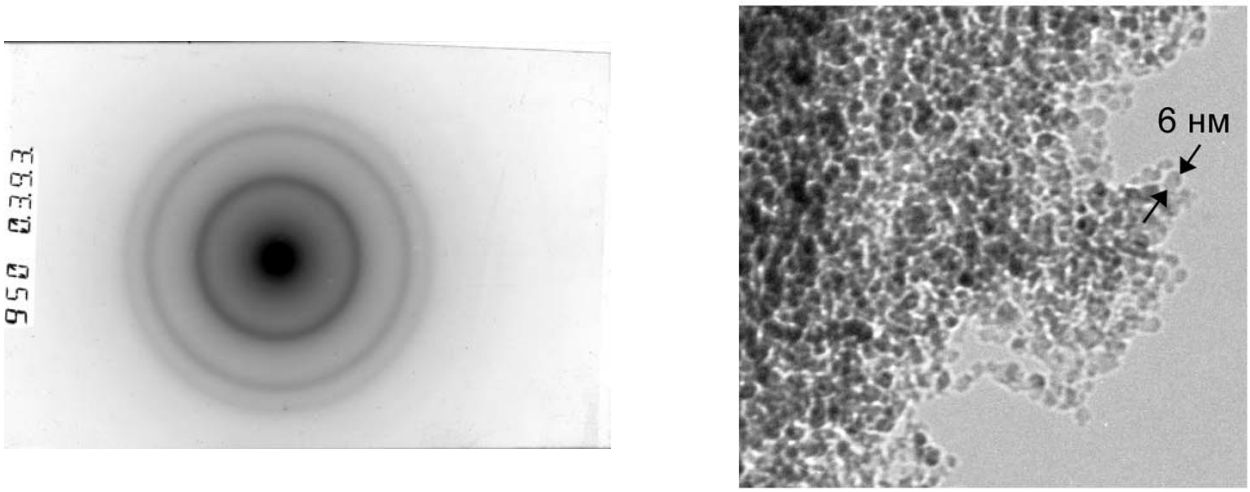

Figure S8. TEM image (right) and electron diffraction pattern (left) of the DND particles recovered from the cold trap during drying of DND samples. Compare with Figures 1 and S7

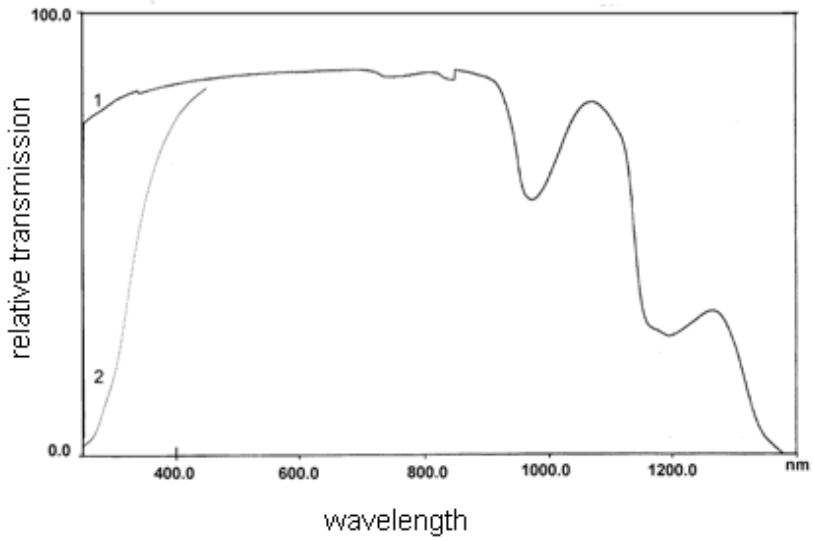

Figure S9. UV spectra of pure water (1) and "diamond water" (2).

Table S2. Sound velocity (m/s) in "diamond water" (W_D) and pure water (W_o) *vs* temperature

t°C	W_D	W_o	t°C	W_D	W_o	t°C	W_D	W_o
22	1490.6	1487.5	14	1463.6	1460.6	6	1434.5	1429.7
21	1488.4	1485.2	13	1460.8	1458.3	5	1430.7	1427.5
20	1485.6	1482.8	12	1458.3	1453.2	4	1426.7	1424.8
19	1482.4	1477.5	11	1454.1	1450.9	3	1424.1	1423.5
18	1479.0	1475.1	10	1450.3	1445.9	2	1422.7	1421.4
17	1477.3	1471.1	9	1447.8	1441.4	1	1420.6	1413.7
16	1471.8	1467.6	8	1442.6	1439.1	0	1419.7	1409.7
15	1469.2	1465.2	7	1438.3	1434.1			

Table S3. Dielectric permittivity of “diamond water”: temperature dependence

t°C	ε·×10^6	t°C	ε×10^6	t°C	ε	t°C	ε
22	2.16	16	1.98	10	1.76	4	$1.54 \cdot 10^6$
21	2.13	15	1.94	9	1.73	3	$4.10 \cdot 10^5$
20	2.08	14	1.89	8	1.70	2	$2.59 \cdot 10^5$
19	2.06	13	1.87	7	1.66	1	$3.56 \cdot 10^4$
18	2.02	12	1.84	6	$1.62 \cdot 10^6$	0	$5.5 \cdot 10^3$
17	2.00	11	1.81	5	$1.59 \cdot 10^6$	−1	$2.95 \cdot 10^4$